Evidence for Increased Low Force Cross-Bridge Population in Shortening Skinned Skeletal Muscle Fibers: Implications for Actomyosin Kinetics

Hiroyuki Iwamoto
Department of Physiology, School of Medicine, Teikyo University, Tokyo 173, Japan

ABSTRACT The dynamic characteristics of the low force myosin cross-bridges were determined in fully calcium-activated skinned rabbit psoas muscle fibers shortening under constant loads (0.04–0.7 × full isometric tension P_o). The shortening was interrupted at various times by a ramp stretch (duration, 10 ms; amplitude, up to 1.8% fiber length) and the resulting tension response was recorded. Except for the earlier period of velocity transients, the tension response showed nonlinear dependence on stretch amplitude; i.e., the magnitude of the tension response started to rise disproportionately as the stretch exceeded a critical amplitude, as in the presence of inorganic phosphate (P_i). This result, as well as the result of stiffness measurement, suggests that the low force cross-bridges similar to those observed in the presence of P_i (presumably A·M·ADP·P_i) are significantly populated during shortening. The critical amplitude of the shortening fibers was greater than that of isometrically contracting fibers, suggesting that the low force cross-bridges are more negatively strained during shortening. As the load was reduced from 0.3 to 0.04 P_o, the shortening velocity increased more than twofold, but the amount of the negative strain stayed remarkably constant (~3 nm). This insensitiveness of the negative strain to velocity is best explained if the dissociation of the low force cross-bridges is accelerated approximately in proportion to velocity. Along with previous reports, the results suggest that the actomyosin ATPase cycle in muscle fibers has at least two key reaction steps at which rate constants are sensitively regulated by shortening velocity and that one of them is the dissociation of the low force A·M·ADP·P_i cross-bridges. This step may virtually limit the rate of actomyosin ATPase turnover and help increase efficiency in fibers shortening at high velocities.

INTRODUCTION

In the generally accepted scheme of actomyosin reaction in contracting muscle, a quaternary complex of actin, myosin, ADP, and inorganic phosphate (P_i) is formed (A·M·ADP·P_i) after hydrolysis of ATP on myosin (for reviews see, e.g., Hibberd and Trentham, 1986; Goldman, 1987). This A·M·ADP·P_i intermediate may be further divided into several substates, and apparently one of them should represent the low force attached cross-bridges that subsequently isomerize into force-producing forms. Existence of such low force cross-bridges has been suggested from the observation that P_i has different effects on isometric tension and fiber stiffness, which is usually taken to reflect the number of attached cross-bridges. Application of P_i has been reported to reduce isometric tension but reduce the fiber stiffness to a lesser extent (Hibberd et al., 1985; Kawai et al., 1987; Brozovich et al., 1988; Dantzig et al., 1992; Martyn and Gordon, 1992; Iwamoto, 1995). These results suggest the presence of low force cross-bridges that contribute to fiber stiffness but do not support tension.

A similar situation is also found in shortening muscle fibers. Increasing the shortening velocity toward its maximum (V_{max}) reduces the tension level toward zero, but again, it reduces the stiffness to a lesser extent. It has been reported that approximately 40% of isometric stiffness still remains at V_{max} in frog muscle fibers (Julian and Sollins, 1975; Julian and Morgan, 1981; Tsuchiya et al., 1982; Ford et al., 1985). X-ray diffraction studies also show that the number of cross-bridges that are attached to or stay in the vicinity of the actin filament is virtually unchanged until the shortening velocity comes close to V_{max} (Podolsky et al., 1976; Sugi et al., 1978; Huxley, 1979). The difference between the levels of tension and stiffness may be explained by recently revealed large filament compliance (Huxley et al., 1994; Wakabayashi et al., 1994; Kojima et al., 1994; see also Goldman and Huxley, 1994), but the stiffness remaining at a zero tension level and the x-ray results are not readily explained by the filament compliance. The relative insensitiveness of the number of attached cross-bridges to shortening velocity may be explained by either or both of the following mechanisms: (1) the average force per force-producing cross-bridge (presumably A·M·ADP) is reduced and/or (2) the fraction of the low force cross-bridge population (presumably A·M·ADP·P_i) is increased. The second possibility is naturally expected as a consequence of the increased dissociation rate of force-producing A·M·ADP and A·M complexes during shortening. The purpose of the present study is to test the second possibility, i.e., whether there exists an increased number of the low force A·M·ADP·P_i cross-bridges during shortening. To achieve this, comparison of the mechanical characteristics should be made between shortening fibers and fibers contracting isometrically in the presence of P_i.

In the previous study we examined the dynamic properties of the low force A·M·ADP·P_i cross-bridges in the pres-

Received for publication 21 February 1995 and in final form 25 May 1995.
Address reprint requests to Dr. Hiroyuki Iwamoto, Department of Physiology, School of Medicine, Teikyo University, 2–11-1 Kaga, Itabashi-ku, Tokyo 173, Japan. Tel.: 813-3964-1211x2151; Fax: 813-5375-8789; E-mail: iwamoto@po.iijnet.or.jp.

0006-3495/95/09/1022/14 $2.00

ence of P_i by applying ramp stretches of various amplitudes to skinned rabbit skeletal muscle fibers (Iwamoto, 1995). In the presence of 20 mM P_i, the tension response to a ramp stretch (duration, 10 ms) started to increase disproportionately as the stretch amplitude exceeded ~4 nm/half-sarcomere. This nonlinear behavior was observed even when the stretch was prolonged to more than 100 ms. From these results it was postulated that the low force A·M·ADP·P_i cross-bridges start to support force when they are extended beyond the critical distance of ~4 nm (possibly through accelerated force-producing isomerization) and that their dissociation rate constant is small under isometric conditions (~10 s^{-1}).

The same strategy may be used to detect and characterize the putative low force cross-bridges during shortening. If shortening of fibers increases the number of the low force A·M·ADP·P_i cross-bridges, sudden stretches of shortening fibers should elicit nonlinear mechanical responses as observed in the presence of P_i. In the present study, rabbit skeletal muscle fibers were allowed to shorten under constant loads (0.04–0.7 × isometric force P_o), and ramp stretches of various amplitudes (up to 1.8% of fiber length L_o) were applied immediately after the shortening was terminated.

In the present paper we will show that shortening fibers exhibit nonlinear responses to stretch similar to those in the presence of P_i, just as expected for an increased population of the low force A·M·ADP·P_i cross-bridges. In addition, detailed comparison of the nonlinearity between shortening and isometrically contracting fibers suggested that the dissociation of the low force A·M·ADP·P_i cross-bridges seems to be greatly accelerated by shortening. The dissociation rate could reach 300 s^{-1} at V_{max}. As will be discussed, this large velocity dependence of the dissociation rate constant will have profound implications for the kinetics and energetics of the actomyosin ATPase reaction in fibers and will provide clues to a number of unanswered questions about how the studies on muscle fibers, isolated proteins, and in vitro motility assay systems are related to each other.

MATERIALS AND METHODS

The materials and solutions were prepared as described previously (Iwamoto, 1995). Briefly, small bundles (two to four fibers) of skinned fibers were prepared from rabbit psoas muscle and mounted on the experimental apparatus. In a few cases single fibers were prepared to obtain a clear sarcomere diffraction pattern. The force transducer (AE801, Senso-Nor, Horten, Norway) had a resonant frequency of 3.5 kHz in solution and an elastic modulus of 2 N/mm. The servo motor, capable of completing a step length change within 0.5 ms, was General Scanning G120D (Watertown, MA) with a CX-660 controller (General Scanning). The relaxing solution had the following composition: 80 mM potassium propionate, 10 mM EGTA, 5 mM $MgCl_2$, 4 mM Na_2-ATP, 20 mM phosphocreatine (Sigma Chemical Co., St. Louis, MO), 20 U/ml creatine phosphokinase (Sigma), and 20 mM imidazole (pH 7.2). In the preactivating solution [EGTA] was reduced to 0.1 mM. For the full activating solution, 10~10.2 mM $CaCl_2$ was added to the relaxing solution. In some experiments, 6% (w/v) dextran (Sigma, average molecular weight = 160,000) was added to all solutions to prevent the filament lattice from swelling. Inclusion of dextran tended to increase fiber stiffness and also isometric tension, especially in the presence of 20 mM P_i. However, the nonlinear feature of the tension response to stretches was not affected. The temperature of the experimental solutions was kept at 3–5°C.

Isotonic shortening

The general experimental setup was also previously described in detail (Iwamoto, 1995). The isotonic shortening was performed by a digital servo isotonic controller. Fibers were activated in the isometric (length control) mode until steady tension was reached (7 s). The controller was then turned to the isotonic (tension control) mode and the fibers were allowed to shorten under a predetermined constant load (0.04–0.7 × P_o). After a period of isotonic shortening (12–250 ms, depending on the load and the kind of experiment), the controller was returned to the isometric mode. The fibers were transferred to the relaxing solution at 9 s from the start of activation. The signal for the ramp stretch was applied to the servo motor at the moment when the isotonic controller was turned from the isotonic to the length control modes. The trial without ramp stretch (control) was interspersed every three to four contractions. The control tension signal was subtracted from the signal with a stretch to obtain the tension response caused by the stretch.

In some experiments fiber stiffness was measured by applying sinusoidal vibrations (frequency, 500 Hz, amplitude, 0.1–0.2% L_op-p) throughout the period of recording. This was achieved by the following procedure. In the first contraction, isotonic shortening was performed in the usual manner and the command signal fed to the servo motor amplifier was stored in a digital memory. In the following contractions, the stored command signal was fed to the servo motor in the length control mode, after adding sinusoidal oscillation signals. The tension in these contractions almost exactly followed the time course of the tension of the first contraction (see Fig. 1).

RESULTS

Time course of fiber length and stiffness during isotonic shortening at 0.3 P_o

After the plateau of the calcium-activated tension was reached, the muscle fibers were released to a load of 0.3 P_o, allowed to shorten for 150 ms, and then held isometric for the rest of the period of contraction. Two upper traces in Fig. 1 show the time courses of length and tension, starting shortly before the isotonic release and including a 150-ms period of isometric contraction after shortening (see lower traces of length and tension for this period). The traces with and without 500-Hz oscillation are superposed.

After the tension was suddenly reduced to 0.3 P_o, the fiber length showed a period of velocity transient before the fiber started to shorten at a constant velocity. The time course of the transient was similar to that reported for living frog single fibers (Civan and Podolsky, 1966), but the transient was more conspicuous. After the fast shortening concomitant with the reduction of tension, the shortening decelerated and reached a plateau lasting 30–40 ms. The shortening accelerated again and an additional small hump was observed in the length record before the final velocity was attained.

The fiber stiffness (the third trace from the top of Fig. 1, filled squares), measured as the amplitude of the tension response to oscillation, decreased slowly during the whole period of the velocity transient and approached a steady level, indicating that the number of attached myosin cross-bridges was decreasing. At 150 ms after the start of shortening, still ap-

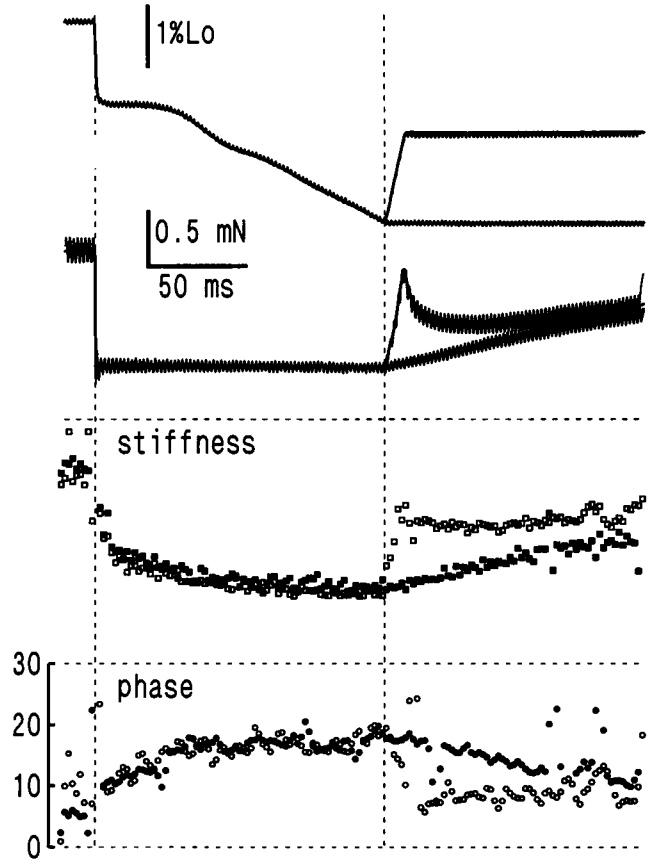

FIGURE 1 Time courses of fiber length, tension, stiffness, and phase lead of tension during isotonic shortening at 0.3 P_o for 150 ms, followed by isometric contraction or a ramp stretch (amplitude, 1.5% L_o; duration, 10 ms). The stiffness and the phase lead of tension over length were measured by applying 500-Hz oscillations. Top trace, length (position output of the servo motor); second from the top, tension. In these two, the records with and without oscillations are superposed. Second trace from the bottom, stiffness (in an arbitrary unit); bottom trace, phase lead (in degrees). Filled symbols indicate isotonic shortening followed by isometric contraction; open symbols indicate shortening followed by a ramp stretch. The stiffness and phase data were taken from three contractions. Two vertical broken lines mark the beginning and the end of the isotonic shortening.

proximately 40% of isometric stiffness remained. This higher stiffness relative to tension is consistent with the previous results for frog muscle fibers (for references see Introduction) and suggests lower average force per cross-bridge or the presence of an increased population of low force cross-bridges, or both. After the shortening was terminated, the stiffness rose slowly.

The phase lead of the tension response to oscillation over length is also shown in Fig. 1 (bottom trace, filled squares). The phase lead of tension in this frequency range (500 Hz) can be ascribed to some rapid configurational fluctuation of myosin heads while attached (Iwamoto, 1995). Before the isotonic shortening was initiated, the phase lead was less than 10° but increased during the velocity transient with a time course approximately in a mirror image of the stiffness decrease. After the shortening was terminated, the phase gradually decreased toward its original level. The behavior of the stiffness and phase are similar to those in the presence of 20 mM P_i, in which isometric tension is reduced to 30% of control (Iwamoto, 1995).

Effect of stretch on the stiffness of shortening fibers

Fig. 1 also shows the time courses of length, tension, fiber stiffness, and phase lead when a stretch (amplitude, 1.5% L_o; duration, 10 ms) was applied immediately after the termination of shortening under a load of 0.3 P_o for 150 ms (the upper traces of length and tension after the end of shortening; open symbols for stiffness and phase). Upon stretch, the stiffness (open squares) increased to a value close to the pre-release level. At the same time, the phase lead of tension (open circles) decreased below 10°. These responses of the stiffness and phase are very similar to those of fibers contracting isometrically in the presence of 20 mM P_i (Iwamoto, 1995). These observations suggest that the population of low force cross-bridges similar to those in the presence of P_i (presumably A·M·ADP·P_i) is increased in shortening fibers.

Comparison of tension response to stretch under various experimental conditions

To make a more systematic comparison between the properties of fibers shortening at 0.3 P_o and fibers contracting isometrically in the presence or absence of P_i, single specimens were stretched by 1.2% under these three conditions and fiber stiffness was also measured at the same time. The results are shown in Fig. 2. When normalized to the pre-stretch level of tension, the responses of the fibers after shortening (Fig. 2 *a*) and in the presence of P_i (Fig. 2 *b*) were greater than that in the absence of P_i (Fig. 2 *c*). A 1.2% stretch of shortening fibers or fibers in the presence of P_i increased fiber stiffness and decreased the phase lead to levels close to those of isometric contraction in the absence of P_i (Table 1). The changes of fiber stiffness and phase lead upon stretch were greatest in shortening fibers and smallest in the fibers in the absence of P_i. The increase of fiber stiffness and the decrease of phase lead upon stretch were highly significant in all three experimental conditions (mostly $P < 0.001$), but the phase lead after stretch after shortening or in the presence of P_i was not significantly different from the level before stretch in the absence of P_i ($P > 0.05$).

Tension response to stretch of various amplitudes

The stiffness measurement (Figs. 1 and 2) showed that low force cross-bridges similar to those in the presence of P_i are significantly populated during shortening. It is of interest, therefore, to test whether the tension response to stretch of

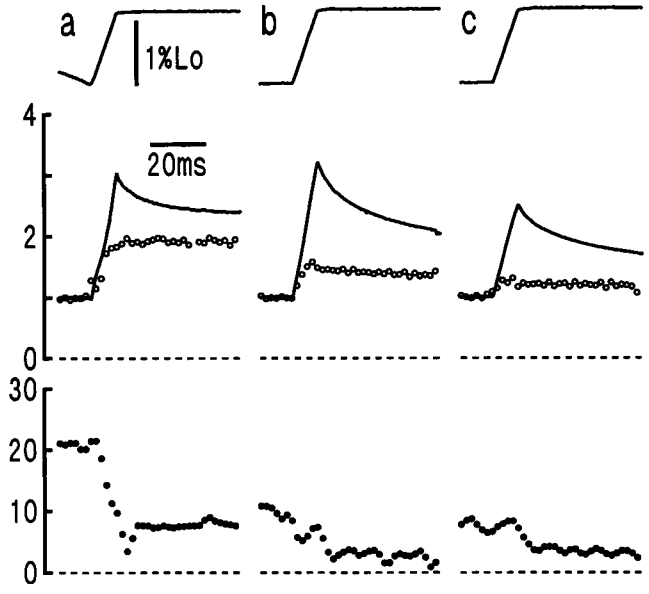

FIGURE 2 Changes of tension, stiffness, and phase lead induced by a stretch (amplitude, 1.2% L_o; duration, 10 ms). The stiffness and the phase lead of tension over length were measured by applying 500-Hz oscillations. Top trace, length (position output of the servo motor); middle traces, tension (solid line) and stiffness (circles); bottom trace, phase lead (in degrees). Tension and stiffness are normalized so that the values before application of stretch are 1. (*a*) After shortening at 0.3 P_o for 150 ms; (*b*) 20 mM added P_i; (*c*) control (no added P_i). Dextran (6% w/v) was added to solutions. In the presence of dextran, the isometric tension in the presence of P_i was approximately 50% of control and the tendency of the tension decay to be accelerated after a stretch was not very conspicuous at this amplitude (1.2%).

shortening fibers also shows nonlinear amplitude dependence as observed in the presence of P_i.

Fig. 3 shows superposed traces of overall length, sarcomere length, and tension of a single fiber to which stretches of various amplitudes (0.3 to 1.5% L_o in 0.3% steps) were applied immediately after shortening at 0.3 P_o for 150 ms. Although the sarcomere length reflects the length change applied at an end of the fiber, the traces for the responses are unevenly spaced, indicating that the dependence of the tension response on stretch amplitude is nonlinear. The greatest increment of the tension response was seen for the stretch amplitudes between 0.6 and 1.2% L_o.

To describe the nonlinearity more quantitatively, the peak magnitude of the tension response is plotted against the stretch amplitude, after subtraction of the control record, i.e., without stretch (top curve in Fig. 4). As in the presence of P_i (Iwamoto, 1995), this stretch amplitude-response curve shows a flexion point between 0.3 and 0.6% L_o, above which its slope is increased. The similarity of the shape of the stretch amplitude-response curves to that recorded in the presence of P_i (see Fig. 6 *c*; see also Fig. 5 in Iwamoto, 1995) provides further support for the idea that the fraction of the low force A·M·ADP·P_i cross-bridges is increased in shortening fibers as well. The tension response started to level off as the stretch amplitude exceeded 1.2% (in the case of P_i, only data for stretches up to 1.2% were taken (Iwamoto, 1995)). Because of this leveling off, the curve has a sigmoidal appearance. These features of the stretch amplitude-response curve were not affected by inclusion of 6% (w/v) dextran, except that the leveling off was somewhat alleviated (data not shown).

Effect of varying duration of shortening on the linearity of tension response

At 150 ms after the start of shortening at 0.3 P_o, the velocity transient was over and the fibers seemed to have reached a steady state. The data in Fig. 3 show that by this time the population of the low force cross-bridges has increased substantially. Then a question arises as to how fast the low force cross-bridges are accumulated after the start of shortening. To answer this question, the duration of the isotonic shortening was varied in the range between 12 and 150 ms.

In Fig. 4, the stretch amplitude-response curves are shown for various shortening durations in a decreasing order from above. The sigmoidal feature of the curve as seen for 150-ms shortening is already clear for 75- and 50-ms shortening, although the steady state has not been established within these periods. After shortening for 37 ms (the end of the plateau phase of the velocity transient), the sigmoidal feature is less obvious. After shortening for 25 ms (the middle of the plateau phase of the velocity transient), the curve is almost linear. After shortening for 12 ms, the tendency seen for shortening longer than 50 ms is completely reversed; i.e., the slope of the curve decreases with increasing stretch amplitude. The slope increases again at very large amplitudes. The reason for this reversal is unclear, but at least it can be said that there would be few low force cross-bridges in this period.

In the previous paper (Iwamoto, 1995), the presence of a flexion point was interpreted to mean that the low force cross-bridges start to support force when the stretch amplitude exceeds this point. If this holds for shortening fibers, then it is expected that the slope of the curve below the flexion point reflects mainly the number of force-producing cross-bridges, and the slope above the flexion point the total cross-bridges (low force plus force-producing). It is of interest, then, to follow the time courses of these slopes with the progress of shortening. In Fig. 5, the data in Fig. 4 are replotted to show such time courses. The slope of the curve for stretches between 0 and 0.3% L_o ($\angle_F$, open circle) decreases monotonically as the shortening is prolonged. The slope of the curve between 0.6 and 0.9% L_o ($\angle_{LF}$, filled circle) initially increases with increasing duration and, after a peak at 50 ms, shows a tendency to decrease gradually. For shortening of 50 ms or longer, the $\angle_{LF}$ is approximately twice as large as the $\angle_F$. The $\angle_{LF}$ exhibits a clear dip at 75 ms. When the $\angle_{LF}$ was determined for each fiber bundle, its value at 75 ms was significantly lower than those at 50 and 100 ms ($P < 0.001$ and $P < 0.02$, respectively; $n = 15$ for

TABLE 1 Effect of 1.2% stretch on stiffness and phase

Condition	Relative stiffness			Phase (°)	
	Before stretch	After stretch	Increment (%)	Before stretch	After stretch
0.3 P_o	0.48 ± 0.02	0.89 ± 0.03	88 ± 2	18.8 ± 2.6	6.4 ± 2.3
20 mM P_i	0.69 ± 0.02	1.01 ± 0.01	47 ± 2	12.1 ± 2.3	4.7 ± 1.7
0 mM P_i	1.00	1.21 ± 0.02	21 ± 2	6.0 ± 3.2	1.8 ± 3.1

Data are expressed as Mean ± SD (n = 5). The stiffness was normalized to the level before stretch at 0 mM P_i of the same specimen. Dextran (6% w/v) was included.

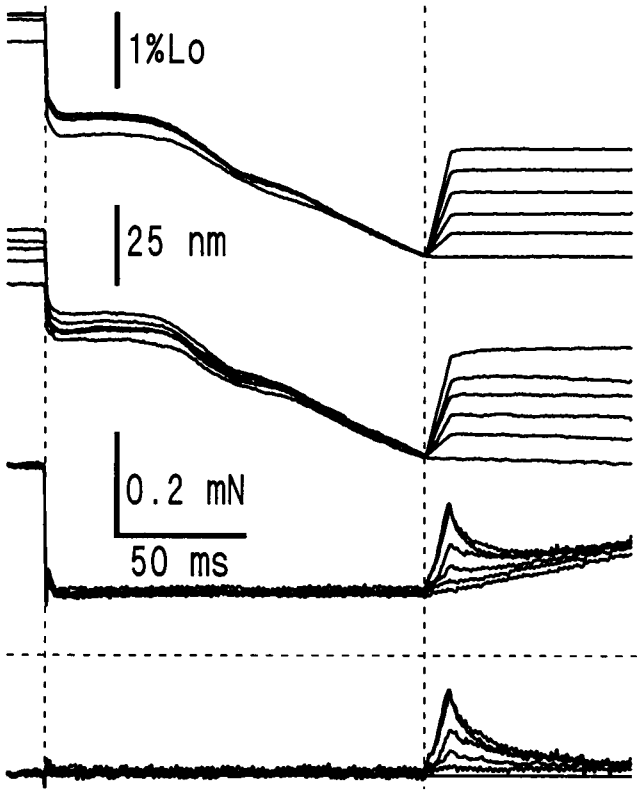

FIGURE 3 Tension responses to stretches (duration, 10 ms) of different amplitudes, applied to a single fiber preparation after shortening at 0.3 P_o for 150 ms. Tension responses to stretches ranging from 0.3 to 1.5% L_o (in a 0.3% step) are superposed. Top traces, overall fiber length (position output of the servo motor); second traces from the top, sarcomere length (position of the first order He-Ne laser reflection); third traces, tension; bottom traces, tension after subtraction of the control record (without ramp stretch). Note that the sarcomere length change is proportional to the amplitude of the length change applied to an end of the fiber, whereas the magnitude of the tension response is not.

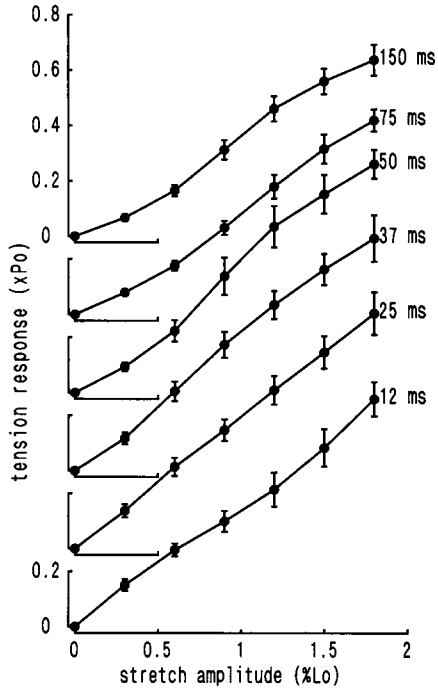

FIGURE 4 Stretch amplitude-response curves, showing dependence of the tension response to stretch on stretch amplitude. Stretches were applied after shortening at 0.3 P_o for various durations. The duration of shortening is marked to the right of each curve. The magnitude of the peak tension response is divided by isometric tension P_o after subtraction of the control record (without ramp stretch). Mean ± SD (n = 6~15). The curves are vertically offset for clarity.

50 ms, 14 for 75 ms, and 3 for 100 ms). Thus, it seems unlikely that this dip is an artifact. This timing (75 ms) coincides with the second hump observed in the velocity transient (see Fig. 1), and may be related to some synchronized behavior of cross-bridges.

The results shown in Figs. 4 and 5 suggest that the low force cross-bridges are not generated immediately after the onset of shortening but are accumulated gradually in the earlier period of the velocity transient. The process could involve some synchronized events until the fiber settles to a steady state.

Detailed analysis of the nonlinear stretch-response curves for 0.3 P_o and other loads

In the stretch amplitude-response curves in Fig. 4, the flexion point seems to lie between 0.3 and 0.6% L_o, but a 0.3% increment of stretch does not provide enough resolution to determine the flexion point accurately. For this reason, the dependence of the tension response on stretch amplitude was examined in greater detail by varying stretch amplitudes with an increment of 0.15% L_o instead of 0.3%. The same analyses were also made for loads other than 0.3 P_o, to test whether the value of the flexion point is affected by shortening velocity.

The fibers were allowed to shorten at 0.04 P_o for 40 ms, 0.1 P_o for 50 ms, 0.3 P_o for 150 ms, 0.5 P_o for 200 ms, and 0.7 P_o for 250 ms. These times were needed for the fibers to

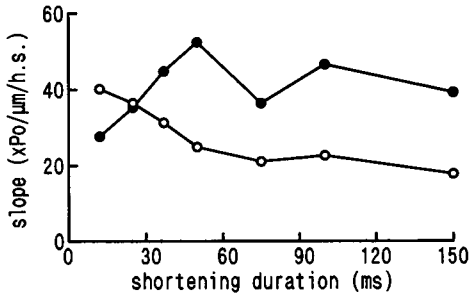

FIGURE 5 Dependence of the slopes of the stretch amplitude-response curve (Fig. 4) on the duration of shortening. The slope of the segment between 0 and 0.3% L_o (○, denoted in text as $\angle_F$) and that between 0.6 and 0.9% L_o (●, denoted in text as $\angle_{LF}$) are taken from Fig. 4, except for those for 100 ms (data from three specimens). Data are expressed as a multiple of isometric tension P_o per 1-μm sliding per half-sarcomere.

start shortening at constant velocities. Fig. 6 shows the results of such analyses on fibers shortening at 0.3 P_o (*a*) and 0.1 P_o (*b*) together with the analyses on fibers held isometric in the presence (*c*) and absence (*d*) of 20 mM P_i. Two linear parts are clearly recognized in all of the stretch amplitude-response curves, including that for isometric contraction without added P_i (Fig. 6 *d*; upon close examination, this tendency is also seen in Fig. 5 of the previous report (Iwamoto, 1995)). This means that a small amount of low force cross-bridges exists in fibers held isometric even in the absence of P_i. The slopes of the two linear parts are determined by least-squares linear regression. The two groups of filled circles in Fig. 6, corresponding to stretch amplitudes below and above the flexion point, respectively, represent the data used for the regression. The center of the flexion point is defined as the crossing point of the two regression lines. The transition of the curve from one linear part to the other is gradual, indicating that the value of the flexion point is distributed along the axis of stretch amplitude. To estimate the distribution of the flexion point, the entire curve was fitted to a convolution of the combined linear function and a Gaussian function, as follows:

$$y(x) = f(x) \otimes \exp(-\ln(2) \times x^2/w^2),$$

where

$$f(x) = \angle_F x \qquad (x < x_{flex}),$$

and

$$f(x) = \angle_{LF}(x - x_{flex}) + \angle_F x_{flex} \qquad (x \geq x_{flex}).$$

The parameter x represents the amount of stretch per half-sarcomere, x_{flex} the center of the flexion point (it will be simply referred to as flexion point), and $\angle_F$ and $\angle_{LF}$ the slopes below and above the flexion point, respectively. The constant w represents the half-width at the half-maximum of

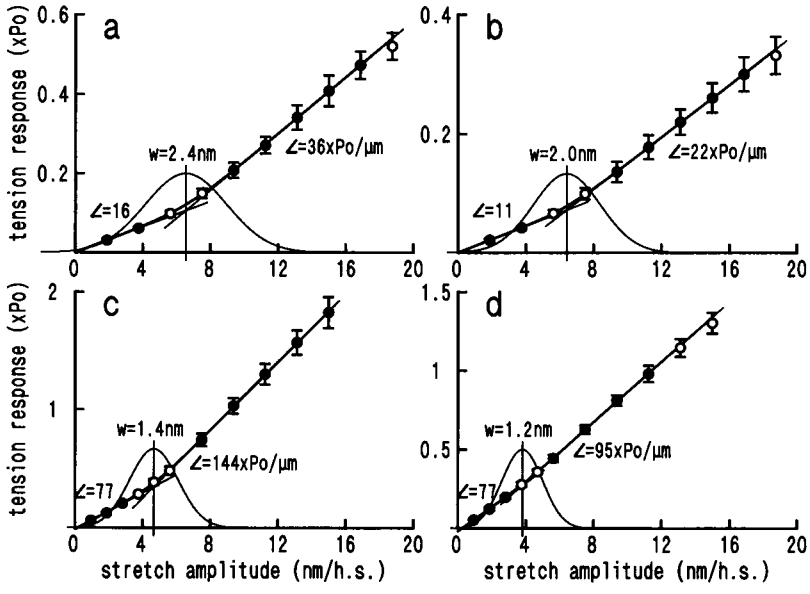

FIGURE 6 Stretch amplitude-response curves at various loads. (*a*) 0.3 P_o; duration of shortening, 150 ms; (*b*) 0.1 P_o, 50 ms; (*c*) stretch applied during isometric contraction in the presence of 20 mM P_i; (*d*) stretch applied during isometric contraction in the absence of added P_i. Curves are similar to those in Fig. 4, but the measurements were made every 0.15% or in some cases (data in *c* and *d*) 0.075% L_o and plotted against the distance per half-sarcomere. Data are expressed as mean ± SD (n = 6). The groups of filled circles below and above the flexion point represent data used to obtain least-squares regression of the two linear parts (thin straight lines) of the whole curve. The value of each slope is expressed as a multiple of P_o per micron per half-sarcomere and indicated near the corresponding part of the curve. The vertical line represents the flexion point, defined as the crossing point of the two linear parts. The bell-shaped curve (thin line) is the best-fit Gaussian function used to fit the entire stretch amplitude-response curve. The number on its top is the half-width at the half-maximum (w; see text). The fitted stretch amplitude-response curve, calculated as the convolution of the combined linear functions and the Gaussian function (see text for detail), is drawn in a thick line.

the Gaussian function and can be regarded as an approximate measure of the distribution of the flexion point. The symbol ⊗ represents convolution. The fitting procedure was to determine the two linear parts by linear least-squares regression and then to scan the value w until the squared error reached a minimum.

The slopes of the linear parts ($\angle_F$ and $\angle_{LF}$) of the stretch amplitude-response curve are plotted against the load in Fig. 7 *a*. The slope above the flexion point ($\angle_{LF}$, filled circles) decreases almost linearly as the load is decreased. The slope below the flexion point ($\angle_F$, open circles) shows nonlinear dependence on the load. Except for the isometric condition, $\angle_{LF}$ is almost twice as large as $\angle_F$.

The flexion point of the curve for shortening at 0.3 P_o is 6.6 nm/half-sarcomere (h.s.) and its distribution w is 2.4 nm/h.s. (Fig. 6 *a*). These values are greater than the corresponding values for isometric contraction (Fig. 6 *c*, 3.8 nm/h.s. and 1.2 nm/h.s., respectively). The greater value of flexion point suggests that the low force cross-bridges during shortening are more (2.8 nm/h.s.) negatively strained than during isometric contraction. The distribution of the cross-bridges along the fiber axis, as estimated from the value w, also seems to be greater than during isometric contraction. The values of the flexion point and w for shortening at 0.1 P_o (Fig. 6 *b*, 6.1 nm/h.s. and 2.0 nm/h.s., respectively) are not very different from those at 0.3 P_o.

The values of the flexion point and w at loads ranging between 0.04 P_o and 1 P_o (isometric) are summarized in Fig. 7 *b*. The value of the flexion point (filled circles) shows the greatest increase when the load is reduced from 1 P_o to 0.7 P_o, and the value increases only modestly as the load is reduced further. The flexion point at loads below 0.5 P_o is around 6.5 nm/h.s. This constancy of the flexion point is striking, as it means that the amount of the negative strain (~3 nm) is insensitive to shortening velocity. This implies that the dissociation of the low force cross-bridges is accelerated almost in proportion to the shortening velocity. At 0.3 P_o, for example, the shortening velocity was approximately 260 nm/h.s./s. Then the average negative strain of 2.8 nm/h.s. implies that the apparent dissociation rate constant of the low force cross-bridges is approximately 90 s^{-1} (260/2.8). This value is already much higher than reported previously for the fibers isometrically contracting in the presence of P_i (10 s^{-1}; Iwamoto, 1995). As the maximal shortening velocity obtained from the force-velocity relation is ~900 nm/h.s./s (see Fig. 9 *b*), the ~3-nm negative strain means a dissociation rate constant of ~ 300 s^{-1}.

The distribution of the flexion point w (open circles) also increases as the load is reduced and approaches a value of ~2 nm/h.s.

In fibers contracting isometrically in the presence of 20 mM P_i (Fig. 6 *c*), the values for flexion point and w were 4.5 and 1.6 nm/h.s., respectively. These values are slightly larger than those in the absence of P_i (Fig. 5 *d*). The $\angle_{LF}$ (0.14 P_o/nm/h.s.) was approximately twice as large as the $\angle_F$ (0.08 P_o/nm/h.s.).

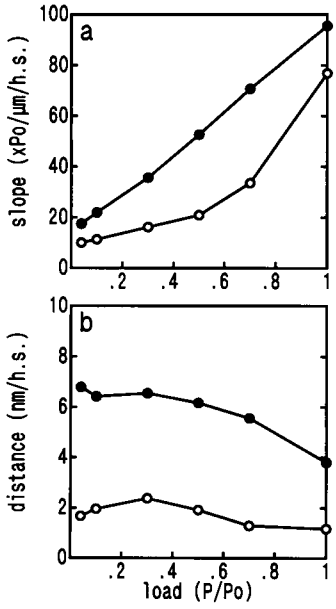

FIGURE 7 Fitted parameters of the stretch amplitude-response curve, as shown in Fig. 6., as functions of load. (*a*) Slopes of the two linear parts: ○, the slope of the part below the flexion point ($\angle_F$); ●, the slope above the flexion point ($\angle_{LF}$). Data are expressed as a multiple of isometric tension P_o per micron per half-sarcomere. Each point was taken from a stretch amplitude-response curve determined from six specimens. (*b*) Flexion point and its distribution: ●, median flexion point; ○, its distribution, i.e., the half-width at the half-maximum (w) of the fitted Gaussian function.

Tension response to faster stretches applied immediately after shortening

The marked insensitiveness of the flexion point to load or velocity, as shown in Fig. 7 *b*, can be most easily explained by the accelerated dissociation of the low force cross-bridges. Alternatively, however, it could also be explained if a large number of low force cross-bridges are quickly formed in a very short period (<10 ms) after the shortening is terminated. If that were true then there would be few low force cross-bridges during shortening. To test this possibility, 1-ms (instead of 10-ms) stretches were applied immediately after the termination of shortening at 0.3 P_o for 150 ms.

Fig. 8 *a* shows the tension responses to 0.3 and 0.6% stretches. Unlike the case of the 10-ms stretch, the peak magnitudes of the responses seem to be proportional to the stretch amplitude. At first glance, this result seems to be at odds with the expectation that the low force cross-bridges are present during shortening. However, such a linear relationship was observed not only for stretches applied immediately after the termination of shortening but also 10 ms after the termination of shortening (Fig. 8 *b*) or during isometric contraction in the presence of 20 mM P_i (Fig. 8 *c*).

Although the time course of tension decay after the completion of stretch cannot be simply fitted to a sum of a small number of exponentials, it does seem to consist of fast

and slow components. After shortening or in the presence of P_i, the slow component was recruited substantially by a 0.6% stretch but not by a 0.3% stretch. As a result, the tension response remaining at 10 ms from the onset of stretch is not proportional to the amplitude of stretch (as can be seen at the end of the records in Fig. 8, *a–c*). In contrast to these conditions, the slow component was recruited by both 0.3 and 0.6% stretches applied during isometric contraction in the absence of P_i (Fig. 8 *d*), so that the response remaining at the end of the record is proportional to the amplitude.

These results are best explained if the force-producing cross-bridges show both fast and slow components at any stretch amplitude but the low force cross-bridges show the slow component only after they are stretched beyond the critical distance. During slow 10-ms stretches, the fast decaying component would be effectively filtered out because the period of stretch is long enough to allow the fast decaying component, which is insensitive to the states of cross-bridges, to decay off. This gives a rationale for using 10-ms stretches to detect selectively the slow component of the response. As the nonlinear slow component was already observed in the first 1 ms from the end of the shortening, it is likely that most of the nonlinear response observed with 10-ms stretches originated from the low force cross-bridges that had already existed during shortening.

DISCUSSION

Effect of filament compliance

The following discussion is made on an assumption that most of the compliance of the fibers resides in the cross-bridges (Ford et al., 1981). Recently, however, several x-ray diffraction and micromechanics studies have shown that both actin and myosin filaments are more compliant than previously considered (Huxley et al., 1994; Wakabayashi et al., 1994; Kojima et al., 1994). It is suggested that, during full isometric tetanus of the frog muscles, as much as 70% of the total compliance of muscle fibers could reside in the filaments (Wakabayashi et al., 1994). Therefore, it would be necessary to assess the effect of filament compliance on the present results. The full isometric tension per cross-sectional area under the present experimental conditions ($\sim 1.2 \times 10^5$ N/m^2; see Iwamoto, 1995) is about one-half of that for frog muscles. However, the increased lattice constant due to the skinning procedure makes the stress per filament comparable to that of intact frog muscles. Huxley et al. (1994) estimated that a total of 2 nm of strain originates from the extension of filaments at an isometric plateau. The present study showed that a stretch of isometrically contracting fibers by the critical distance (3.8 nm/h.s.) results in an approximately 20% increase of tension level. Thus, an extension of 0.4 nm (2 × 0.2) should originate from the filaments, and the real critical distance is estimated to be 3.4 nm/h.s. During shortening at near-zero load, on the other hand, most of the compliance is expected to reside in the cross-bridges. Thus, the uncorrected amount of negative strain of the cross-bridges during shortening is an underestimate, and the corrected negative strain at near-zero load is estimated to be 6.6 − 3.4 = 3.2 nm/h.s (vs. 2.8 nm/h.s. before correction). This correction is small (<20%) and it is therefore considered that the conclusions drawn from the present experiments are basically not affected.

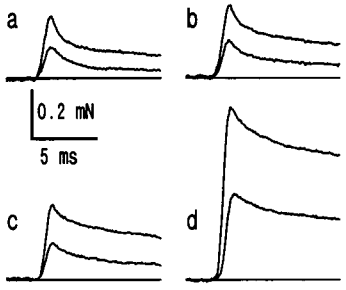

FIGURE 8 Tension responses to fast stretches (duration, 1 ms) applied to a specimen contracting under different conditions. Responses to 0.3 and 0.6% L_o stretches are superposed after subtraction of the control record (without stretch). (*a*) Responses to stretch applied immediately after shortening at 0.3 P_o for 150 ms. (*b*) Responses to stretch applied after the fibers shortened at 0.3 P_o for 150 ms and were held isometric for 10 ms. (*c*) Response to stretch applied during isometric contraction in the presence of 20 mM P_i. The isometric tension was approximately 30% of that in the absence of added P_i. (*d*) Response to stretch applied during isometric contraction in the absence of added P_i. Note that in *a– c*, the magnitude of the tension response is almost proportional to the amplitude of stretch at its peak but not at the end of the record (10 ms from the onset of stretch).

Presence of low force A·M·ADP·P_i cross-bridges in shortening fibers

In the present study, we examined the dynamic characteristics of the cross-bridges during shortening by applying a 10-ms ramp stretch and 500-Hz oscillations. In support of the previous results (e.g., Julian and Sollins, 1975; Podolsky et al., 1976), the present stiffness measurement suggested that more cross-bridges exist in shortening fibers than expected from the tension level. Two mechanisms may lead to this different sensitivity of the tension level and the number of attached cross-bridges to velocity, i.e., lower average force per force-producing cross-bridge and an increased fraction of low force cross-bridge population. Explanations of the higher stiffness level are often made on the basis of only the former mechanism. However, the present results showed that the shortening fibers are in many respects similar to the fibers contracting isometrically in the presence of P_i, and these similarities are not readily explained by the reduced average force per force-producing cross-bridge.

The first of these similarities is that the phase lead of tension over length during 500-Hz oscillation is large and is reduced upon application of a ramp stretch (duration, 10 ms; amplitude, 1.2 or 1.5% L_o). The second similarity is the nonlinear dependence of the tension response on the amplitude of the ramp stretch. The slope of the stretch amplitude-

response curve doubles as the stretch amplitude exceeds a critical amplitude. Another observation related to these similarities is that the tension response to a fast ramp stretch (1 ms) seemed to consist of two components, the slower component being recruited only by larger stretches. All of these types of behavior are observed both in shortening fibers and in fibers contracting isometrically in the presence of P_i, but much less conspicuously in fibers contracting isometrically in the absence of P_i (Figs. 2, 6, and 8).

These similarities suggest that, during shortening, a considerable fraction of the attached cross-bridges are in the form of low force A·M·ADP·P_i species. It is considered, therefore, that the relative insensitiveness of the total number of cross-bridges is the combined effect of the reduced average force per force-producing cross-bridge and an increased population of the low force A·M·ADP·P_i cross-bridges.

Alignment of low force cross-bridges along filament

The stretch amplitude-response curves have a relatively well defined flexion point, the distribution of which is limited to a few nanometers as judged from the half with w of the Gaussian function (Fig. 5). This suggests that the low force cross-bridges are well aligned along the filament axis. During isometric contraction (Fig. 5 *d*), w was only ~1 nm. This value is remarkably smaller than the axial repeat of the myosin molecules along the myosin filament, 14.3 nm. If the low force cross-bridges isomerize to a force-producing form without dissociating from actin, the small w means that the force-producing cross-bridges are also aligned to the same extent. Thus, all the attached cross-bridges are expected to be in good register with respect to an axial repeat of 14.3 nm, which provides the basis for the increased intensity of the 14.3-nm meridional x-ray reflexion during isometric contraction (Huxley et al., 1981).

During shortening, it is expected that w will increase because the low force cross-bridges that attach at different times will be continuously displaced. This was actually observed, and w increased with increasing velocity (Fig. 6 *a*). However, w leveled off as the velocity was increased further, just as the critical amount of stretch. This supports the idea that the low force cross-bridges which are negatively strained by more than ~3 nm dissociate very quickly, thus limiting the spread of the axial distribution.

The force-producing cross-bridges probably dissociate more slowly than the low force cross-bridges, and accordingly, the spread of their axial distribution is expected to be greater. If the force-producing cross-bridges dissociate 10 times slower than the low force cross-bridges (see the following calculation), the interaction distance (distance of sliding over which a force-producing cross-bridge stays attached to actin whether or not it produces positive force) is estimated to be ~30 nm. This value agrees with the estimate of 40 nm by Higuchi and Goldman (1991).

Increased dissociation rate constant of low force cross-bridges during shortening and its consequences

Besides the similarities of shortening fibers and fibers held isometric in the presence of P_i, the present study also revealed a consistent difference between these fibers. That is, the critical amount of stretch needed to elicit greater tension response was invariably greater in shortening fibers. This increased critical amount would be best explained by the following mechanism.

During shortening, an attached cross-bridge is continuously being negatively strained, i.e., strained in a direction opposite to the way of force generation. Thus, for a low force cross-bridge to isomerize to a force-producing form, it should be stretched by a greater amount (critical amount under isometric condition plus amount of negative strain). As the fibers shorten further, the low force cross-bridges are more negatively strained. When the negative strain reaches a value of ~3 nm, the dissociation of the low force cross-bridges is accelerated, so that the average negative strain will not exceed this value. This mechanism also ensures that the overall dissociation rate of the low force cross-bridges is increased in proportion to the shortening velocity.

The estimated rate of the dissociation of the low force cross-bridges increases from 10 s^{-1} under isometric conditions (Iwamoto, 1995) to 300 s^{-1} for unloaded shortening. The possible consequences of this increased dissociation rate constant are discussed below in detail.

Cross-bridge distributions and energetics estimated by simple calculations

To study the consequences of the increased dissociation rate constant of the low force cross-bridges, it would be useful to construct a simple actomyosin reaction scheme, on the basis of which the behavior of each intermediate can be predicted after making appropriate assumptions. Such a reaction scheme of the actomyosin ATPase cycle may be written as follows:

$$D \underset{k_-}{\overset{k_+}{\rightleftharpoons}} L \xrightarrow{f} F \xrightarrow{g} D$$

Scheme 1

where D represents the dissociated states (M·ATP and M·ADP·P_i), L the low force associated state (A·M·ADP·P_i), and F the force-producing states (A·M·ADP and A·M). For simplicity, only the transition between D and L is assumed to be reversible (forward and reverse rate constants are denoted as k_+ and k_-, respectively). The rate constants of the transition from L to F and F to D are denoted as f and g, respectively. The distribution of cross-bridges among these states, force, energy rate, and efficiency are calculated by using a simple calculation procedure by Iwamoto et al.

(1990). The procedure was originally developed to reproduce the principal feature of Huxley's 1957 model. It was assumed that, with increasing shortening velocity, the dissociation rate constant g increases linearly and the force per cross-bridge decreases linearly. An additional assumption introduced in the present calculation is that the L cross-bridges do not contribute to tension at all. As in Huxley's 1957 original model, it is assumed that the dissociation of an F cross-bridge is tightly coupled to a single ATP breakdown. The detail of the calculations is given in the Appendix.

Fig. 9 shows the result of the calculation. In Fig. 9 *a*, the reverse rate constant of association, k_-, is independent of shortening velocity. In Fig. 9 *b*, k_- increases linearly with increasing shortening velocity (10 s^{-1} during isometric contraction and 310 s^{-1} during shortening at V_{max}) whereas other parameters are left unchanged. Introducing such velocity dependence to k_- affects many aspects of the kinetics and energetics of muscle contraction. With increasing velocity, the fraction of the F cross-bridges (densely stippled area) decreases in both cases, but it does so more steeply when k_- is velocity dependent. The fraction of the L cross-bridges (lightly stippled area) increases monotonically with increasing velocity when k_- is constant, but it starts to decrease as the velocity approaches its maximum when k_- is velocity dependent. Thus, introducing velocity dependence to k_- results in a smaller fraction of total attached cross-bridges ($L + F$) at high shortening velocities. Other properties affected by introducing velocity dependence to k_- are (1) the force-velocity curve (solid line), (2) the total energy rate (coarsely broken line), and (3) efficiency (finely broken line). The curvature of the force-velocity curve is increased where k_- is velocity dependent. This corresponds to a smaller value of the parameter a/P_o in Hill's (1938) hyperbolic equation. For direct comparison with real force-velocity data, the velocities of the fibers used to obtain results in Figs. 6 and 7 are also plotted in Fig. 9 *b*. In the present calculation, the total energy rate is directly proportional to the fraction of the L cross-bridges. Accordingly, it shows a maximum at an intermediate velocity and decreases as the velocity approaches the V_{max} where k_- is velocity dependent. Introducing velocity dependence to k_- improves the efficiency in the low load range.

In a sense, the curves in Fig. 7 *a* would be equivalent to the cross-bridge distribution among different states as shown in Fig. 9, if one makes an assumption that the slope of the stretch amplitude-response curve below the flexion point ($\angle_F$) reflects only the number of force-producing cross-bridges whereas the slope above the flexion point ($\angle_{LF}$) represents total associated cross-bridges. The curves in Fig. 7 *a* differ from those of Fig. 9 *b* in many respects; e.g., the curve of $\angle_F$ in Fig. 7 *a* is convex downward. This disagreement may be because the assumptions made here are too simple. In addition, at high velocities, some of the low force cross-bridges could have escaped detection because of their accelerated dissociation kinetics. Apart from

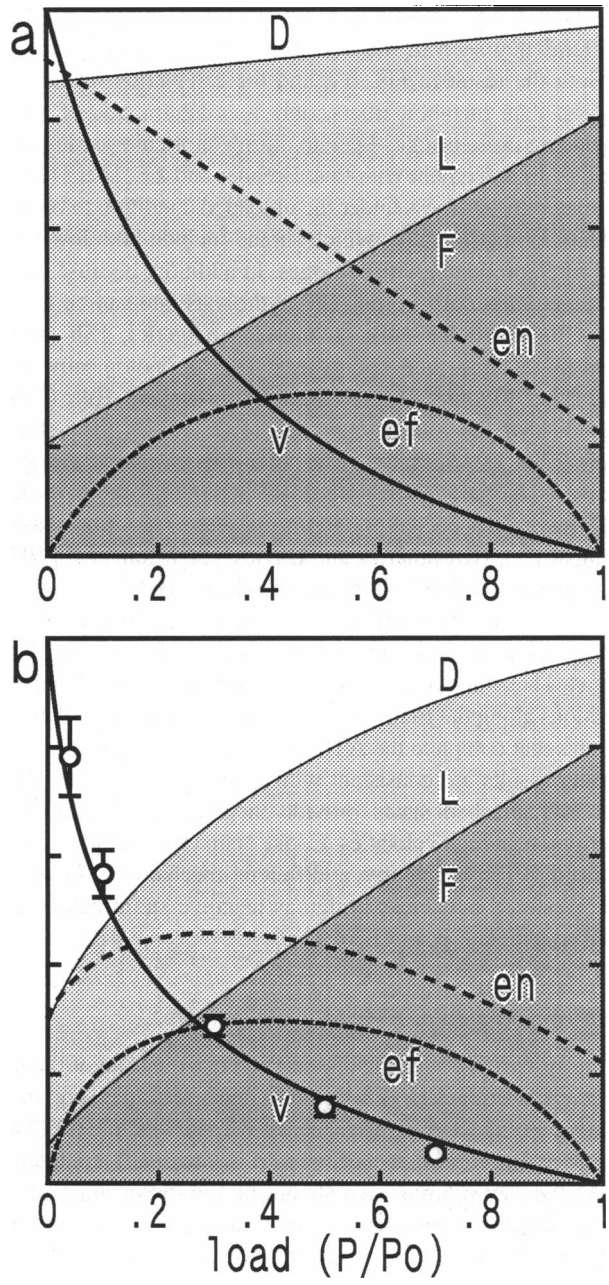

FIGURE 9 Distribution of the cross-bridges among three states (dissociated D, low force L, and force-producing F states), shortening velocity, energy liberation (ATPase) rate, and efficiency as functions of load, as calculated from Scheme 1. The basic assumptions for calculations are that the force per force-producing cross-bridge decreases linearly and the dissociation rate constant of F cross-bridges (g) increases linearly with increasing velocity. In *a*, the reverse rate constant for the association in the L state (k_-) is assumed to be independent of velocity. In *b*, k_- is assumed to increase in proportion to velocity, as suggested from the present results. White, lightly stippled, and densely stippled areas indicate the proportion of the cross-bridges in D, L, and F states, respectively. v, velocity; en, energy liberation rate; ef, efficiency. The last two are in arbitrary units. The values of the parameters used for calculation are given in the Appendix. The open circles with error bars represent the real force-velocity data from specimens from which data in Figs. 6 and 7 were taken (mean ± SD; n = 6). The data are plotted relative to the maximal shortening velocity (V_{max}) obtained by fitting them to Hill's (1938) hyperbolic function. The fitted parameters are: a/P_o = 0.18; b = 0.13 L_o/s; V_{max} = 0.71 L_o/s (hyperbola not shown).

these details, the calculation in Fig. 9 *b* seems to reproduce the tendency seen in the real fibers shown in Fig. 7 *a*.

Both the result in Fig. 6 *a* and the calculation in Fig. 9 *b* suggest that, in rabbit fibers, only a small fraction of force-producing cross-bridges operate during shortening at high velocities. In agreement with this, Brenner and Eisenberg (1986) estimated the stiffness under the unloaded condition to be only 20% of isometric value, which should include both low force and force-producing cross-bridges. In addition, because of the increased value of k_-, the ATP hydrolysis rate can be low at V_{max}. In his initial work on muscle energetics, Hill (1938) showed that the total energy rate rises monotonically with increasing velocity. More recently, however, Hill (1964) showed that the total energy rate levels off as the velocity approaches its maximum. The total energy rate could even decrease as the velocity approaches its maximum; a low ATPase rate has been reported for muscles or myofibrils shortening at V_{max} (Kushmerick and Davies, 1969; Rall et al., 1976; Homsher et al., 1981; Ohno and Kodama, 1991). To accommodate the leveling off of the energy rate, Huxley (1973) introduced a two-step attachment process to his original 1957 model. These steps were assumed to occur in a limited range of positions along the filament, thus limiting the number of cross-bridges that complete the ATPase cycle at high velocities. The present results are consistent with those of Huxley (1973) in that two attached states provide the basis for the reduced energy rate at high velocities. Cooke et al. (1994) explained the reduced ATPase rate by a different mechanism, in which energy stored in a cross-bridge as negative strain can be utilized to generate positive force.

Rate-limiting step of ATPase cycle in fibers

In the system in which the dissociation rate constant of the low force cross-bridges (k_-) is velocity dependent, the shortening velocity is expected to influence the way in which the ATPase rate is regulated in muscle fibers. In isometrically contracting fibers the rate limiting step should be the dissociation of the force-producing cross-bridges (F) or a step associated with it (e.g., the release of ADP from an A·M·ADP state; see Dantzig et al., 1991). The dissociation of the force-producing cross-bridges is probably facilitated by the sliding-induced relief of their strain, and during isometric contraction, this is restricted as a result of the geometrical constraints posed by the organized assembly of proteins. When the fiber shortens at its maximal velocity, the force-producing cross-bridges will be allowed to relieve their strain and thus the dissociation rate constant g will increase. At the same time, however, the low force cross-bridges attached to the same actin filament would also be brought to a configuration favorable for dissociation, thus increasing the reverse rate constant, k_-. As a result, the equilibrium constant for the low force cross-bridge formation (k_+/k_-) will be reduced and this step will now have major influence in limiting the overall rate of reaction (k_{cat}). In the system of isolated proteins (acto-subfragment 1, acto-heavy meromyosin, etc.), no such geometrical constraint exists, allowing the A·M·ADP complex to assume a configuration favorable for dissociation without increasing k_-. Then both dissociation of the A·M·ADP complex and the formation of the low force complex will be fast, and the overall rate will be determined almost exclusively by the force-producing isomerization ($k_{cat} \approx f$). This idea seems to be consistent with the observation by Brenner and Eisenberg (1986) that the ATPase rate in isolated proteins is correlated with the rate of force-producing isomerization (f) measured as the rate of tension redevelopment after unloaded shortening and a restretch (this amount is actually $f + g$, but can be approximated to f where $f \gg g$). The rate-limiting step in isolated proteins could be either the hydrolysis step (Rosenfeld and Taylor, 1984; Hibbert and Trentham, 1986) or the isomerization between two A·M·ADP·P_i substates (A·M·ADP·P_iI and A·M·ADP·P_iII; Stein et al., 1984), but at high ionic strengths the hydrolysis step is accelerated (Ma and Taylor, 1994). Should the scheme proposed by Stein et al. (1984) apply to the present results, the low force A·M·ADP·P_i would correspond to their A·M·ADP·P_i^I, as the formation of the low force A·M·ADP·P_i should precede the rate-limiting transition (A·M·ADP·P_i^I to A·M·ADP·P_i^{II}). As no evidence is available for a direct coupling between the hydrolysis step and the low force cross-bridge formation, we need to include another A·M·ADP·P_i substate that represents the weak binding, rapid equilibrium form.

Taken together, the entire ATPase reaction in the fibers that appeared in Scheme 1 may be rewritten to a working scheme as follows:

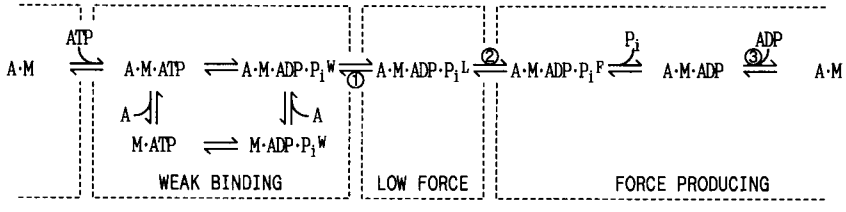

Scheme 2

In this scheme, the intermediates in the box labeled WEAK BINDING correspond to the D cross-bridges in Scheme 1. At physiological ionic strengths, they are expected to be predominantly in dissociated forms. Three A·M·ADP·P_i substates are assumed, i.e., A·M·ADP·P_i^W, A·M·ADP·P_i^L, and A·M·ADP·P_i^F, corresponding to the D, L, and F cross-bridges, respectively. The reverse rate constant of the A·M·ADP·P_i^L formation (step 1) corresponds to k_- in Scheme 1. The rate constant of step 2 corresponds to f. This is a primary factor that limits the rate of isometric tension development and possibly limits the ATPase rate in isolated proteins. The rate constant of ADP release (step 3) corresponds to g. The rate constants of steps 1 and 3 are sensitively regulated by shortening velocity, and the rate constant of step 2 is increased upon stretch.

To summarize, the mechanism proposed here seems to explain the present results of mechanics as well as many of the published observations. In muscle fibers, the contractile proteins are organized into a regular array of filaments. In the proposed mechanism, this organized array of proteins causes an increase of k_- during shortening, thereby preventing the low force and weak binding intermediates from proceeding to force-producing forms. The same organized array would pose another restriction to the ATPase cycle during isometric contraction by limiting the rate of ADP release. As the system of isolated proteins is free of such geometrical constraints, it may be regarded as a model for a system in which ATPase turnover can be maximized rather than a model for isometric fibers or fibers shortening at V_{max}.

Implications for in vitro motility assay studies

The accelerated dissociation of the low force cross-bridges would ensure a reduced rate of ATP hydrolysis during shortening at high velocities. In this system, the filaments are driven by relatively few force-producing cross-bridges and the rest of the cross-bridges are prevented from entering the force-producing cycle. This is a kind of negative cooperativity made possible by the organized array of proteins.

At first glance, this idea seems to be inconsistent with the results of in vitro motility assay studies. Harada et al. (1990) showed that actin filaments only 40 nm long can slide on a myosin-coated surface as fast as longer filaments. In this case, the system can contain a very limited number of molecules and the actin filament would diffuse away unless each myosin head spends most of the ATPase cycle time interacting with actin. However, their observation is easily reconciled with the mechanism proposed here. Having fewer available molecules means greater chances of having no force-producing cross-bridges at all. Nevertheless, the actin filament will stay attached because there are still a number of low force cross-bridges. As soon as the actin filament loses all of its force-producing cross-bridges and stops sliding, the negative cooperativity will be lost; i.e., k_- will fall sharply. Then force-producing cross-bridges will be immediately formed from the rapidly growing pool of low force cross-bridges and the filament will resume its sliding. It is therefore predicted that the ATPase rate for very short filaments is higher than that for longer filaments.

CONCLUSION

The present study suggests that the fraction of the low force A·M·ADP·P_i cross-bridge population is increased during shortening as well as in the presence of P_i. The previous (Iwamoto, 1995) and the present observations lead us to postulate that the low force A·M·ADP·P_i cross-bridges are strain sensitive in two ways: (1) when the fiber is stretched, their isomerization to a force-producing form is accelerated, and (2) when the fiber is shortening, their dissociation rate is increased almost in proportion to the shortening velocity. This dual strain sensitivity gives a basis to the previously proposed idea that the low force cross-bridges act as ratchets, i.e., they provide resistance to stretch but do not act as an internal load during shortening (Iwamoto, 1995). This is especially true for fibers shortening in the presence of P_i, inasmuch as P_i does not reduce V_{max} (Cooke and Pate, 1985). The idea of dual strain sensitivity would be useful in explaining some of the energetic aspects of muscle contraction. The stretch-induced isomerization of the low force cross-bridges will result in an instantaneous increase of the force-producing cross-bridges. Under these conditions cross-bridges are considered to have a low turnover rate (Curtin and Davies, 1973) and the muscle will be able to resist stretch with a greater force with smaller energy expenditure.

The mechanism of this dual strain sensitivity at a submolecular level is yet to be elucidated and the recently determined crystal structures of actin (Kabsch et al., 1990) and myosin head (subfragment-1; Rayment et al., 1993b) may be useful in doing this. It is suggested that contractile force is produced through progressive strengthening of the binding of myosin to actin toward a rigor-like state (Geeves, 1991). In terms of crystal structure, this force generation is suggested to be a sequential, multistep process that starts with interaction sites in the lower domain of the 50-kDa segment of the myosin head, followed by involvement of the sites in the upper domain (Rayment et al., 1993a). Then the low force cross-bridge may represent an early stage of this process and involve relatively few of these interactions. The cross-bridge will have a large degree of freedom of motion, hence little force and large fluctuation (large phase lead of tension upon oscillation). A stretch beyond a critical distance may suddenly bring most of the interaction sites into contact and the freedom of motion will be lost and hence there will be a greater resistance to length change. The shortening of the fiber will bring the low force cross-bridges just in the opposite direction, decreasing the number of interactions further and facilitating dissociation. The range of position along the filament in which these molecular events occur would be less than 10 nm, i.e., well within the size of the myosin head (~17 nm).

In isometric contraction, the later stages of the actomyosin ATPase cycle (e.g., release of ADP) may play a major

role in limiting the rate of ATP hydrolysis. During shortening at increasing velocities, the step of the association in a low force form may play an increasingly important role in determining the rate of ATP hydrolysis. One may say that the ATPase turnover in fibers is sensitively regulated through these two key steps. In short, studying the properties of the low force cross-bridges is crucial in understanding the kinetics and energetics of actomyosin interaction in contracting muscles, isolated proteins, and in vitro motility systems from a unified point of view.

APPENDIX

The distribution of cross-bridges among three states, force, energy rate, and efficiency were calculated for scheme 1 in the Discussion. Let L, F, and D represent the fractions of the cross-bridges attached in the states L, F, and D, respectively. In the steady state, the time derivatives of L, F and D are 0. Then,

$$dL/dt = k_+D - (k_- + f)L = 0 \quad (1)$$

$$dF/dt = fL - gF = 0 \quad (2)$$

$$dD/dt = (k_- + f)D - k_+L = 0 \quad (3)$$

$$L + F + D = 1. \quad (4)$$

By solving these equations, one can obtain

$$L = k_+g/(k_+f + g(k_+ + k_- + f)) \quad (5)$$

$$F = k_+f/(k_+f + g(k_+ + k_- + f)). \quad (6)$$

The energy rate in the steady state is defined as gF. From Eq. 2., it is clear that this is equal to fL. If f is fixed and its reverse reaction can be ignored, the energy rate is proportional to L.

The force per cross-bridge (in the state F) is assumed to decrease linearly with increasing velocity. Then the normalized fiber tension P/P_o is expressed as

$$P/P_o = F(1 - V/V_{max})/F_o, \quad (7)$$

where V and V_{max} are the shortening velocity and its maximal value, respectively. F_o is the value of F for isometric contraction.

The dissociation rate constant g is assumed to increase linearly with increasing V; i.e.,

$$g = g_o + c_1(V/V_{max}), \quad (8)$$

where c_1 is a constant and g_o is the g for isometric contraction.

The reverse rate constant for the association, k_-, is either constant or velocity dependent, as in the case of g. That is,

$$k_- = k_{-o} + c_2(V/V_{max}), \quad (9)$$

where c_2 is a constant and k_{-o} is the k_- for isometric contraction.

The constants used for the calculation shown in Fig. 9 are as follows (in s^{-1}): $k_+ = 100$, $k_{-o} = 10$, $f = 10$, $g_o = 2$, $c_1 = 30$, and $c_2 = 0$ (Fig. 9 *a*) or 300 (Fig. 9 *b*).

The author expresses his hearty thanks to Prof. H. Sugi for his support of this work.

REFERENCES

Brenner, B., and E. Eisenberg. 1986. Rate of force generation in muscle: correlation with actomyosin ATPase activity in solution. *Proc. Natl. Acad. Sci. USA.* 83:3542–3546.

Brozovich, F. V., L. D. Yates, and A. M. Gordon. 1988. Muscle force and stiffness during activation and relaxation: implications for the actomyosin ATPase. *J. Gen. Physiol.* 91:399–420.

Civan, M. M., and R. J. Podolsky. 1966. Contraction kinetics of striated muscle fibres following quick changes in load. *J. Physiol.* 184:511–534.

Cooke, R., and E. Pate. 1985. The effects of ADP and phosphate on the contraction of muscle fibers. *Biophys. J.* 48:789–798.

Cooke, R., H. White, and E. Pate. 1994. A model of the release of myosin heads from actin in rapidly contracting muscle fibers. *Biophys. J.* 66:778–788.

Curtin, N. A., and R. E. Davies. 1973. Chemical and mechanical changes during stretching of activated frog skeletal muscle. *Cold Spring Harbor Symp. Quant. Biol.* 37:619–626.

Dantzig, J. A., Y. E. Goldman, N. C. Millar, J. Lacktis, and E. Homsher. 1992. Reversal of the cross-bridge force-generating transition by photogeneration of phosphate in rabbit psoas muscle fibres. *J. Physiol.* 451:247–278.

Dantzig, J. A., M. G. Hibberd, D. R. Trentham, and Y. E. Goldman. 1991. Cross-bridge kinetics in the presence of MgADP investigated by photolysis of caged ATP in rabbit psoas muscle fibres. *J. Physiol.* 432: 639–680.

Ford, L. E., A. F. Huxley, and R. M. Simmons. 1981. The relation between stiffness and filament overlap in stimulated frog muscle fibres. *J. Physiol.* 311:219–249.

Ford, L. E., A. F. Huxley, and R. M. Simmons. 1985. Tension transients during steady shortening of frog muscle fibres. *J. Physiol.* 361:131–150.

Geeves, M. A. 1991. The dynamics of actin and myosin association and the cross-bridge model of muscle contraction. *Biochem. J.* 274:1–14.

Goldman, Y. E. 1987. Kinetics of the actomyosin ATPase in muscle fibers. *Annu. Rev. Physiol.* 49:637–654.

Goldman, Y. E., and A. F. Huxley. 1994. Actin compliance: are you pulling my chain? *Biophys. J.* 67:2131–2133.

Harada, Y., K. Sakurada, T. Aoki, D. D. Thomas, and T. Yanagida. 1990. Mechanochemical coupling in actomyosin energy transduction studied by in vitro movement assay. *J. Mol. Biol.* 216:49–68.

Hibberd, M. G., and D. R. Trentham. 1986. Relationships between chemical and mechanical events during muscular contraction. *Annu. Rev. Biophys. Biophys. Chem.* 15:119–161.

Hibberd, M. G., D. R. Trentham, and Y. E. Goldman. 1985. Phosphate release and force generation in skeletal muscle fibers. *Science.* 228: 1317–1319.

Higuchi, H., and Y. E. Goldman. 1991. Sliding distance between actin and myosin filaments per ATP molecule hydrolysed in skinned muscle fibres. *Nature.* 352:352–354.

Hill, A. V. 1938. The heat of shortening and the dynamic constants of muscle. *Proc. R. Soc. Lond. B.* 126:136–195.

Hill, A. V. 1964. The effect of load on the heat of shortening of muscle. *Proc. R. Soc. Lond. B.* 159:297–318.

Homsher, E., M. Irving, and A. Wallner. 1981. High-energy phosphate metabolism and energy liberation associated with rapid shortening in frog skeletal muscle. *J. Physiol.* 321:423–436.

Huxley, A. F. 1957. Muscle structure and theories of contraction. *Prog. Biophys. Biophys. Chem.* 7:255–318.

Huxley, A. F. 1973. A note suggesting that the cross-bridge attachment during muscle contraction may take place in two stages. *Proc. R. Soc. Lond. B.* 183:83–86.

Huxley, H. E. 1979. Time resolved x-ray diffraction studies on muscle. *In* Cross-Bridge Mechanism in Muscle Contraction. H. Sugi and G. H. Pollack, editors. University of Tokyo Press, Tokyo. 391–405.

Huxley, H. E., R. M. Simmons, A. R. Faruqi, M. Kress, J. Bordas, and M. H. J. Koch. 1981. Millisecond time-resolved changes in x-ray reflections from contracting muscle during rapid mechanical transients, recorded using synchrotron radiation. *Proc. Natl. Acad. Sci. USA.* 78:2297–2301.

Huxley, H. E., A. Stewart, H. Sosa, and T. Irving. 1994. X-ray diffraction measurements of the extensibility of actin and myosin filaments in contracting muscle. *Biophys. J.* 67:2411–2421.

Iwamoto, H. 1995. Strain sensitivity and turnover rate of low force cross-bridges in contracting skeletal muscle fibers in the presence of phosphate. *Biophys. J.* 68:243–250.

Iwamoto, H., R. Sugaya, and H. Sugi. 1990. Force-velocity relation of frog skeletal muscle fibres shortening under continuously changing load. *J. Physiol.* 422:185–202.

Julian, F. J., and D. L. Morgan. 1981. Variation of muscle stiffness with tension during tension transients and constant velocity shortening in the frog. *J. Physiol.* 319:193–203.

Julian, F. J., and M. R. Sollins. 1975. Variation of muscle stiffness with force at increasing speeds of shortening. *J. Gen. Physiol.* 66:287–302.

Kabsch, W., H. G. Mannherz, D. Suck, E. F. Pai, and K. C. Holmes. 1990. Atomic structure of the actin:DNase I complex. *Nature.* 347:37–44.

Kawai, M., K. Güth, K. Winnikes, C. Haist, and J. C. Rüegg. 1987. The effect of inorganic phosphate on the ATP hydrolysis rate and the tension transients in chemically skinned rabbit psoas fibers. *Pflügers Arch.* 408:1–9.

Kojima, H., A. Ishijima, and T. Yanagida. 1994. Direct measurement of stiffness of single actin filaments with and without tropomyosin by in vitro nanomanipulation. *Proc. Natl. Acad. Sci. USA.* 91:12962–12966.

Kushmerick, M. J., and R. E. Davies. 1969. The chemical energetics of muscle contraction. II. The chemistry, efficiency and power of maximally working sartorius muscles. *Proc. R. Soc. Lond. B.* 174:315–353.

Ma, Y.-Z., and E. W. Taylor. 1994. Kinetic mechanism of myofibril ATPase. *Biophys. J.* 66:1542–1553.

Martyn, D. A., and A. M. Gordon. 1992. Force and stiffness in glycerinated rabbit psoas fibers: effects of calcium and elevated phosphate. *J. Gen. Physiol.* 99:795–816.

Ohno, T., and T. Kodama. 1991. Kinetics of adenosine triphosphate hydrolysis by shortening myofibrils from rabbit psoas muscle. *J. Physiol.* 441:685–702.

Podolsky, R. J., R. St. Onge, and R. W. Lymn. 1976. X-ray diffraction of actively shortening muscle. *Proc. Natl. Acad. Sci. USA.* 73:813–817.

Rall, J. A., E. Homsher, A. Wallner, and W. F. H. M. Mommaerts. 1976. A temporal dissociation of energy liberation and high energy phosphate splitting during shortening in frog skeletal muscles. *J. Gen. Physiol.* 68:13–27.

Rayment, I., H. M. Holden, M. Whittaker, C. B. Yohn, M. Lorenz, K. C. Holmes, and R. A. Milligan. 1993a. Structure of the actin-myosin complex and its implications for muscle contraction. *Science.* 261:58–65.

Rayment, I., W. R. Rypniewski, B. Schmidt-Base, R. Smith, D. R. Tomchick, M. M. Benning, D. A. Winkelmann, G. Wesenberg, and H. M. Holden. 1993b. Three-dimensional structure of myosin subfragment-1: a molecular motor. *Science.* 261:50–58.

Rosenfeld, S. S., and E. W. Taylor. 1984. The ATPase mechanism of skeletal and smooth muscle acto-subfragment 1. *J. Biol. Chem.* 259: 11908–11919.

Stein, L. A., P. B. Chock, and E. Eisenberg. 1984. The rate-limiting step in the actomyosin adenosinetriphosphatase cycle. *Biochemistry.* 23: 1555–1563.

Sugi, H., Y. Amemiya, and H. Hashizume. 1978. Time-resolved x-ray diffraction from frog skeletal muscle during an isotonic twitch under a small load. *Proc. Jpn. Acad. Sci.* 54B:559–564.

Tsuchiya, T., K. Güth, H. J. Kuhn, and J. C. Rüegg. 1982. Decrease in stiffness during shortening in calcium activated skinned muscle fibers. *Pflügers Arch.* 392:322–326.

Wakabayashi, K., Y. Sugimoto, H. Tanaka, Y. Ueno, Y. Takezawa, and Y. Amemiya. 1994. X-ray diffraction evidence for the extensibility of actin and myosin filaments during muscle contraction. *Biophys. J.* 67: 2422–2435.